Use of a rotating cylinder electrode in corrosion studies of a 90/10 Cu–Ni alloy in 0.5 mol L⁻¹ H₂SO₄ media

J.M. MACIEL[1,2] and S.M.L. AGOSTINHO[1]
[1]*Instituto de Química, Universidade de São Paulo. Av. Prof. Lineu Prestes 748, Caixa Postal 26077, CEP 05508-990, São Paulo – SP, Brazil*
[2]*Presently at: UNIMAR, University of Marilia, Marilia – SP, Brazil, CEP 17515-460*

Abstract

The corrosion of 90/10 Cu–Ni alloy in deaerated 0.5 mol L⁻¹ H₂SO₄ containing Fe(III) ions as oxidant and benzotriazole as inhibitor was studied using a rotating cylinder electrode (RCE). Nonselective dissolution was observed in all experimental conditions investigated. In the absence of Fe(III) ions, the anodic process is diffusion controlled while cathodic process is charge transfer controlled. In contrast, with Fe(III) ions as oxidant, the cathodic process is controlled by diffusion and the anodic process is under charge transfer control. These conclusions were obtained from measurements of open circuit potential as a function of the RCE rotation rate as previously verified for the RDE. Inhibition efficiency evaluated from weight loss and calculated from polarization curves showed good agreement.

List of symbols

A	electrode area (cm^2)
C	concentration (mol L^{-1})
C_{ox}	oxidant concentration (mol L^{-1})
D	diffusion coefficient (cm s^{-1})
D_m	metal ion diffusion coefficient (cm s^{-1})
D_{ox}	oxidant diffusion coefficient (cm s^{-1})
D	electrode diameter (cm)
E_a°	standard potential of the anode (V)
E_c°	standard potential of the cathode (V)
E_{corr}	corrosion potential (V)
F	faradaic constant (C mol^{-1})
i	current density (A cm^{-2})
i_o	exchange current density (A cm^{-2})
I_L	limiting current (A)
k	constant
n	number of electrons involved in a redox process
n_a	number of electrons involved in the anodic process
n_c	number of electrons involved in the cathodic process
R	gas constant (J mol^{-1} K^{-1})
T	absolute temperature (K)
U	electrode peripheric velocity (cm s^{-1})

Greek letters

v_o	corrosion rate in the absence of BTAH
v_i	corrosion rate in the presence of i moles of BTAH
α_a	anodic transfer coefficient
α_c	cathodic transfer coefficient
η	overpotential (V)
Δ_m	weight loss (g)
Δ_t	time interval (s)
θ_1	inhibitor efficiency from weight loss measurements
θ_2	inhibitor efficiency from polarization curves
v	kinematic viscosity (cm^2 s^{-1})

1. Introduction

Copper–nickel alloys with copper as the main component are largely employed when high mechanical strength, good thermal conductivity and good corrosion resistance are required. These alloys are employed in the manufacture of pumps, valves and in tubing of heat exchangers. They are installed in ships and in power plants where large volumes of sea or fresh water, frequently polluted, are employed [1–4]. In such media these alloys show excellent performance but, in some instances, corrosion is observed due to water contamination [5, 6].

The majority of the corrosion studies involving Cu–Ni alloys aim at the characterization of the material in the medium in which it will be used [7–9]. Frequently, the experiments are carried out in such a way that the hydrodynamic aspects of the system are poorly defined.

In corrosion studies, two considerations are relevant to obtain best information: (i) the experimental apparatus employed should reproduce the in service physical and hydrodynamic conditions and (ii) the material under test should be evaluated in the physical form in which it will be used. We have previously described a rotating cylinder electrode (RCE) that meets these

requirements [10]. For this RCE we determined the empirical relationship between limiting current density and rotation rate for a variety of experimental conditions. In turbulent flow, this relationship can be represented by the following equation:

$$I_L = (0.062 \pm 0.016)nFd^{-0.3}v^{-0.344}D^{0.644}$$
$$\times CAU^{(0.747 \pm 0.018)} \tag{1}$$

Benzotriazole ($C_6H_5N_3$, BTAH), is known to be an efficient corrosion inhibitor for copper [11–16], brasses [17, 20], iron and ferrous alloys [21, 22]. With copper, the protection is attributed to a polymeric film of Cu(I)BTA formed on the metal surface [12, 15, 19].

The effect of BTAH in the corrosion of copper and its alloys has been studied in our laboratory [11, 14–18]. These studies were carried out in acidic medium to render the corrosion products soluble, thus preventing growth of surface layers.

In this paper we report some results of corrosion studies of the 90/10 Cu–Ni alloy employing the RCE. The medium studied was deaerated 0.5 mol L^{-1} H_2SO_4, containing Fe(III) ions as oxidant and Benzotriazole (BTAH) as inhibitor. The choice of an acidic medium was based on the reasons stated above. Ferric ions were employed instead of oxygen as oxidant due to the difficulties related to the low solubility and analytical control of the later.

2. Experimental details

All reagents were AR grade, used without further purification. Water was double-distilled, the second distillation being from a $KMnO_4$/NaOH solution. The system employed was a conventional three-electrode cell. A platinum screen and a saturated calomel electrode (SCE) were used as counter and reference electrode, respectively. Polarization curves were obtained with a PEC 1 potentiostat (Aardwark) or with an EG&G PAR 273A potentiostat linked to an AT 386 PC.

The RCE employed was described elsewhere [10]. The alloy studied was a 2.7 cm length, 2.7 cm outer diameter piece of a commercial 90/10 Cu–Ni alloy tubing. The chemical composition is shown in Table 1.

Prior to each experiment, the electrode was sanded with silicon carbide sandpaper (400 and 600 grade), rinsed with water and ethanol and dried with hot air. In weight loss measurements, after surface preparation the electrode was assembled and, at the end of the experiment it was rinsed with double distilled water, ethanol and dried with hot air. Then the active part was weighed. The electrolyte was analysed by atomic

absorption with a Varian model AA1200 spectrophotometer using hollow cathode lamp at the appropriate wavelengths (352 nm for nickel and 249 nm for copper). All experiments were conducted in a water-jacketed cell, thermostated at (25 ± 1) °C.

3. Results and discussion

3.1. *Evaluation of the nonselective character of the corrosion process*

The selective or nonselective character of the alloy dissolution process was investigated using weight loss measurements and chemical analysis of the electrolyte, as explained above. The experiments were conducted in deaerated 0.5 mol L^{-1} H_2SO_4, employing the Cu–Ni RCE under three conditions:
(a) with 8.3×10^{-3} mol L^{-1} Fe(III) ions, at open circuit potential and the electrode rotating at 60 cm s^{-1}
(b) with the RCE rotating at 140 cm s^{-1} and polarized anodically at $+40$ mV, $+80$ mV, $+120$ mV, $+160$ mV and $+200$ mV vs SCE
(c) with the RCE rotating at 60 cm s^{-1} at open circuit, in the presence of 8.3×10^{-3} mol L^{-1} Fe(III) ions and either 0.25×10^{-3} mol L^{-1} or 0.4×10^{-3} mol L^{-1} BTAH.

The results obtained are presented in Table 2. These results show, within experimental error, that the corrosion process is nonselective and that the Cu/Ni ratio in solution matches that of the alloy (90.6/9.4) for all conditions studied.

3.2. *Measurement of corrosion potential as function of RCE rotation rate*

Makrides [23] and Tobias and Nobe [24] studied the relationship between electrode potential and rotation rate. Power and others [25, 26] demonstrated with the rotating disc electrode (RDE) that, from the relationship

Table 1. Chemical analysis of the alloy studied

Element	Cu	Ni	Pb	Fe	Zn	Mn	C	S
Found	88.58	9.23	0.02	1.32	0.11	0.47	0.02	0.01

Table 2. Chemical analysis of the electrolytes from weight loss measurements

Potential	Medium	U /cm s^{-1}	Cu/ Ni ratio*
Open circuit	0.5 mol L^{-1} H_2SO_4 + 8.3×10^{-3} mol L^{-1} Fe(III)	60	92.1 : 7.9
Open circuit	0.5 mol L^{-1} H_2SO_4 + 8.3×10^{-3} mol L^{-1} Fe(III) + 0.25×10^{-3} mol L^{-1} BTAH	60	90.4 : 9.6
Open circuit	0.5 mol L^{-1} H_2SO_4 + 8.3×10^{-3} mol L^{-1} Fe(III) + 0.4×10^{-3} mol L^{-1} BTAH	60	90.3 : 9.7
$\eta = 40$ mV	0.5 mol L^{-1} H_2SO_4	140	89.7 : 10.3
$\eta = 80$ mV	0.5 mol L^{-1} H_2SO_4	140	90.0 : 10.0
$\eta = 120$ mV	0.5 mol L^{-1} H_2SO_4	140	88.9 : 11 : 1
$\eta = 160$ mV	0.5 mol L^{-1} H_2SO_4	140	92.0 : 8.0
$\eta = 200$ mV	0.5 mol L^{-1} H_2SO_4	140	90.1 : 9.9

* Cu/Ni ratio in the alloy: 90.6/9.4

between the corrosion potential (E_{corr}) and rotation rate or the concentration of electroactive species, it is possible to obtain mechanistic information about the corrosion process. Their treatment was based on well established electrochemical concepts such as the mixed potential theory of Wagner and Traud [27], the Nernst and Tafel equations [28] and the Levich equation for the mass transport to a RDE [29]. The model was successfully applied for the case of copper in sulphuric and hydrochloric acid media, with ferric ions as oxidant [11, 16].

We have applied the same reasoning to the RCE with the substitution of the Levich equation by the empirical equation (Equation 1) previously determined [10]. After the appropriate substitution and simplification the following equations are obtained:

(a) Cathodic reaction under diffusion control and anodic reaction under charge transfer control. In this case, E_{corr} depends both on velocity and oxidant concentration according to

$$
\begin{aligned}
E_{corr} = {}& [2.3\,RT/(1 - \alpha_a)n_aF] \log i_o \\
& + [2.3\,RT/(1 - \alpha_a)n_aF] \\
& \times \log(0.062\,n_aFd^{-0.3}v^{-0.334}D^{0.664}) \\
& + [1.72\,RT/(1 - \alpha_a)n_aF] \log U \\
& + [2.3\,RT/(1 - \alpha_a)n_aF] \log C_{ox}
\end{aligned} \tag{2}
$$

(b) Both processes are under diffusion control. In this case, E_{corr} depends only on the oxidant concentration, as

$$
\begin{aligned}
E_{corr} = {}& E_a^\circ + [1.53\,RT/(n_aF) \log(D_{ox}D_m)] \\
& + [2.3\,RT/(n_aF)] \log(n_c/n_a) \\
& + [2.3\,RT/(n_aF)] \log C_{ox}
\end{aligned} \tag{3}
$$

(c) Both processes are under charge transfer control. E_{corr} depends as above, only on the oxidant concentration. That is,

$$
\begin{aligned}
E_{corr} = {}& k + [\alpha_c n_c + (1 - \alpha_a)n_a]^{-1} \\
& + [2.3\,RT/F] \log C_{ox}
\end{aligned} \tag{4}
$$

(d) The cathodic process is under charge transfer control and the anodic one under diffusion control. E_{corr} depends on oxidant concentration with positive slope and on velocity with negative slope, according to the equation:

$$
\begin{aligned}
E_{corr} = {}& k + [2.3\,RT/(\alpha_c n_c + n_a)F] \log C_{ox} \\
& - [1.72\,RT/(\alpha_c n_c + n_a)] \log U
\end{aligned} \tag{5}
$$

When the situation described in (b) or (c) occurs, the cathodic reaction will be under diffusion control if the following condition are met:

(i) E_{corr} is closer to E_a° than to E_c°

(ii) $E_a^\circ - E_c^\circ > 0.3\,\text{V}$

Figure 1 shows the measurements of E_{corr} against U made in the absence and presence of Fe(III) ions. It can be seen that in the absence of the oxidant, on the one hand, the slope is negative and, according to the proposed model, the anodic process is controlled by diffusion and the cathodic process by charge transfer (Equation 5). It can be suggested that due to the presence of traces of oxygen, the formation of an oxide layer on the electrode surface would be controlled by the dissolution of the metal, which is transport dependent. On the other hand, in the presence of Fe(III) ions as oxidant, the slope is positive. In this case, the main processes would be
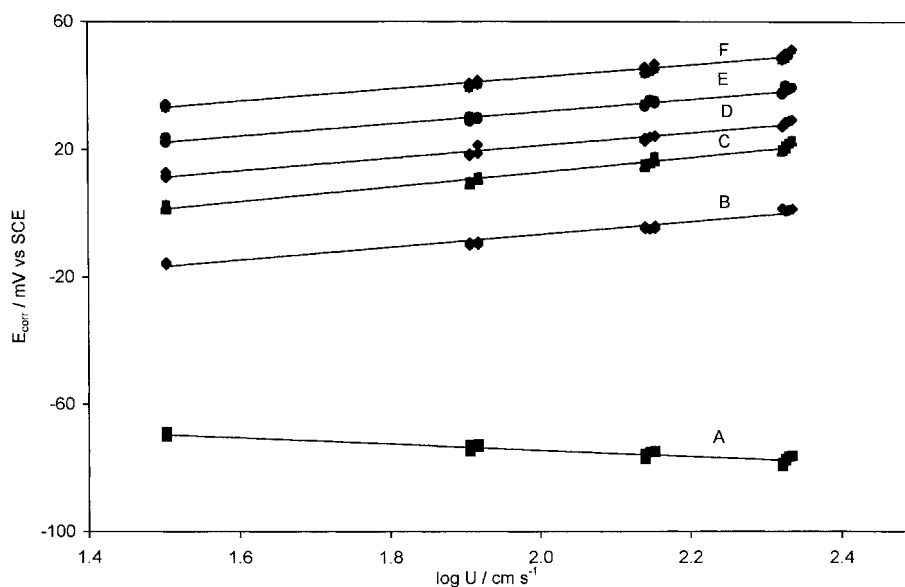

Fig. 1. Relationship between potential, Fe(III) concentration and velocity of the RCE. Medium: 0.5 mol L^{-1} H$_2$SO$_4$. [Fe (III)] / mol L^{-1}: A = 0.0; B = 0.5; C = 1.3; D = 2.9; E = 6.0; F = 12.8.

$$Fe^{3+} + e^- \rightarrow Fe^{2+} \qquad (6)$$

as the cathodic process, under diffusion control, and

$$Cu \rightarrow Cu^{2+} + 2e^- \qquad (7)$$

as the anodic process, under charge transfer control (Equation 2).

3.3. Effect of mass transport on corrosion of 90/10 Cu–Ni alloy in 0.5 mol L^{-1} H_2SO_4/9 × 10^{-3} mol L^{-1} Fe(III) ions in the absence and presence of BTAH

The corrosion rate of the 90/10 Cu–Ni alloy was measured in 0.5 mol L^{-1} H_2SO_4/9 × 10^{-3} mol L^{-1} Fe(III) ions in the absence and presence of various BTAH concentrations. Weight loss results were converted in to current densities through the faradaic law, assuming a nonselective corrosion process. Figure 2 presents the results. The process is mass controlled both in the presence and in the absence of BTAH and obeys the diffusive–convective equation determined for the RCE [10]. The slope decreases as the concentration of the inhibitor grows as a consequence of the formation of an inhibiting film with the corresponding reduction of the electrode area. For 1.7 × 10^{-3} mol L^{-1} BTAH, the inhibition efficiency is close to 100%, within experimental error.

3.4. Potentiodynamic anodic polarization curves

Figure 3 shows potentiodynamic anodic polarization curves of the 90/10 Cu–Ni alloy made for the RCE (rotating at 140 cm s^{-1}) in 0.5 mol L^{-1} H_2SO_4, with and without BTAH. It can be seen that the inhibitive

effect increases as [BTAH] increases, on the entire range of potentials studied.

The corrosion potential (E_{corr}) for the 90/10 Cu–Ni alloy in 0.5 mol L^{-1} H_2SO_4/8 × 10^{-3} mol L^{-1} Fe(III) ions and 0.2 × 10^{-3} mol L^{-1} to 1.0 × 10^{-3} mol L^{-1} BTAH lies in the +120 mV to +150 mV (vs SCE) range.

Table 3 shows the inhibition efficiency (θ) calculated from current density at +150 mV overpotential (vs SCE) and from weight loss as

$$\theta_i = \frac{v_o - v_i}{v_o} \qquad (8)$$

and the corrosion rate values were evaluated from $v_i = i/nF$ or $v_i = \Delta_m/A\Delta_t$ for polarization curves and weight loss experiments, respectively.

Inspection of Table 3 shows good agreement between these values, suggesting that potentiodynamic measurements with the RCE are well suited to simulate the oxidant effect in the absence and presence of BTAH.

4. Conclusions

The 90/10 Cu–Ni alloy showed nonselective dissolution in all H_2SO_4 media studied: (a) in the presence of Fe(III) ions with or without BTAH as inhibitor; and (b) in the presence of BTAH with the electrode polarized to an overpotential value corresponding to that attained by the alloy at open circuit, in the presence of Fe(III) ions and BTAH.

A model previously developed for the rotating disc electrode (RDE) was successfully applied to the rotating cylinder electrode (RCE). With the latter model, it was possible to obtain mechanistic information about the
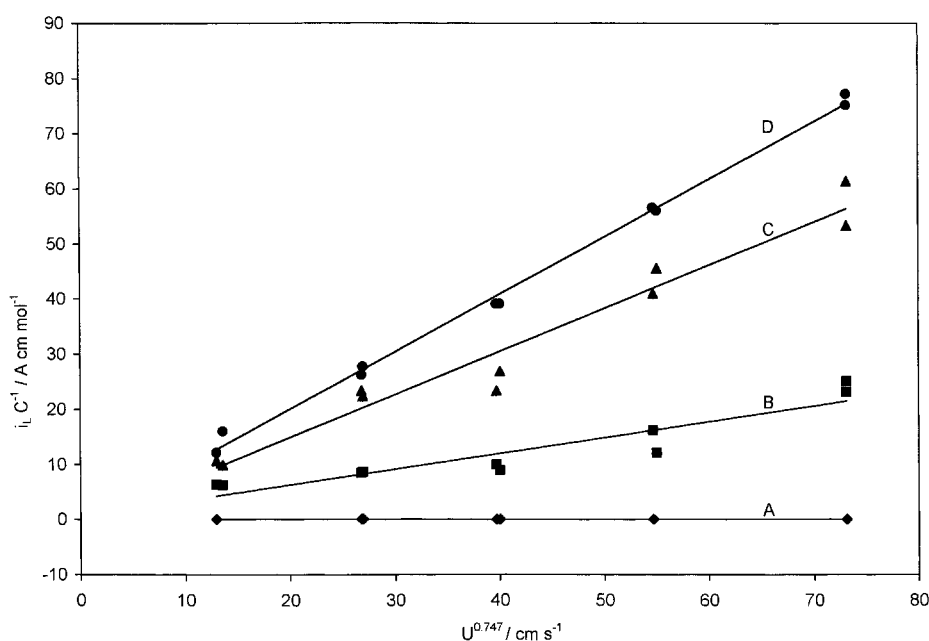

Fig. 2. Corrosion rate of the Cu–Ni as a function of velocity of the RCE and BTAH concentration. Medium: 0.5 mol L^{-1} H_2SO_4/9 × 10^{-3} mol L^{-1} Fe(III). [BTAH]/10^{-3} mol L^{-1}: A = 0.8; B = 0.4; C = 0.2; D = 0.0.
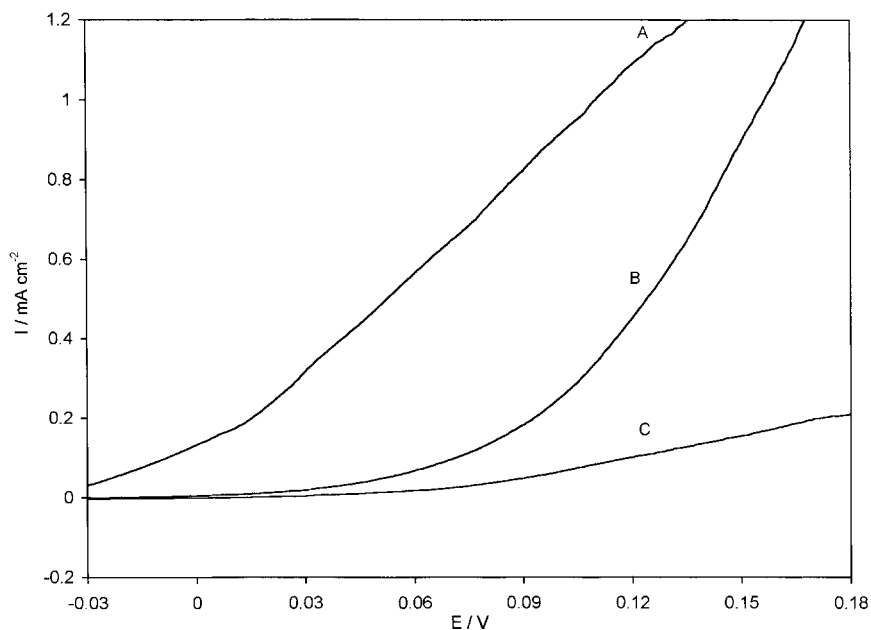
Fig. 3. Potentiodynamic anodic polarisation curves of the 90/10 Cu–Ni alloy in presence of various concentrations of BTAH. Medium: 0.5 mol L^{-1} H$_2$SO$_4$. U = 140 cm s^{-1}. [BTAH]/mol L^{-1}: A = 0.0; B = 0.25; C = 0.97.

Table 3. Inhibitor efficiency measured from weight loss experiments (θ_1) and calculated from anodic polarization curves (θ_2)

[BTAH]/10^{-3} mol dm^{-3}	θ_1	θ_2
0.25	0.42	0.45
0.75	0.81	0.84
0.97	0.89	0.90

alloy dissolution process. It was verified that, while in the absence of Fe(III) ions the anodic process is controlled by diffusion and the cathodic one by charge transfer, in the presence of the Fe(III) ions, the cathodic process is under diffusion control and the anodic one is under charge transfer control.

The inhibitive action of BTAH corresponds to an efficiency of practically 100% for [BTAH] $\geqslant 1.7 \times 10^{-3}$ mol L^{-1}.

Inhibition efficiency calculations from weight loss measurements and polarization curves, showed that potentiodynamic anodic curves obtained with the RCE can be used to simulate the effect of the oxidant on the corrosion of the alloy.

References

1. C. Kato and H. Pickering, *J. Electrochem. Soc.* **131** (1984) 1219.
2. J.G. Parker and J.A. Roscow, *Br. Corros. J.* **16** (1981) 107.
3. R. Francis, *Br. Corros. J.* **22** (1987) 199.
4. R.J.K. Wood, S.P. Hutton and D.J. Schiffrin, *Corros. Sci.* **23** (1983) 223.
5. I. Massiani, S. Petetin, G. Ngo Ngoc and G. Crousier, *Can. J. Chem. Soc.* **131** (1984) 1254.
6. A.M. Beccaria, G. Poggli, P. Traverso and M. Ghiazza, *Corros. Sci.* **32** (1991) 1263.
7. B.C. Syrett, D.D. McDonald and S.S. Wing, *Corrosion* **9** (1979) 409.
8. H.P. Hack and J.P. Gudas, *Mat. Perform.* **19** (1980) 49.
9. D.D. McDonald, B.C. Syrett and S.S. Wing, *Corrosion* **34** (1980) 73.
10. J.M. Maciel and S.M.L. Agostinho, *J. Appl. Electrochem.* **29** (1999) 741.
11. S.F.L. da Costa and S.M.L. Agostinho, *Corrosion* **45** (1989) 472.
12. P.G. Fox, G. Lewis and P.J. Boden, *Corros. Sci.* **19** (1979) 457.
13. G.W. Poling and T. Notoya, *Corrosion* **35** (1979) 193.
14. S.F.L. da Costa, S.M.L. Agostinho, H.C. Chagas and J.C. Rubim, *Corrosion* **43** (1987) 149.
15. S.F.L. da Costa, J.C. Rubim and S.M.L. Agostinho, *J. Electroanal. Chem.* **220** (1987) 259.
16. S.F.L. da Costa and S.M.L. Agostinho, *J. Electroanal. Chem.* **296** (1990) 51.
17. S.F.L. da Costa, S.M.L. Agostinho and J.C. Rubim, *J. Electroanal. Chem.* **295** (1990) 203.
18. S.F.L. da Costa, S.M.L. Agostinho and K. Nobe, *J. Electrochem Soc.* **140** (1993) 3483.
19. P. Gupta, R.S. Chaudari, T.K.G. Namboochiri and B. Prakash, *Br. Corros. J.* **17** (1982) 136.
20. P. Gupta, R.S. Chaudari, T.K.G. Namboochiri and B. Prakash, *Corros. Sci.* **23** (1983) 1361.
21. N. Eldakar and K. Nobe, *Corrosion* **32** (1976) 41.
22. R. Alkire and A. Cangelari, *J. Electrochem. Soc.* **136** (1988) 2441.
23. A.C. Makrides, *J. Electrochem. Soc.* **107** (1960) 869.
24. R.F. Tobias and K. Nobe, *J. Electrochem. Soc.* **122** (1975) 65.
25. G.P. Power and I.M. Ritchie, *Electrochim. Acta* **26** (1981) 1073.
26. G.P. Power, W.P. Staunton and I.M. Ritchie, *Electrochim. Acta* **27** (1982) 165.
27. C. Wagner and W. Traud, *Z. Elektrochem.* **44** (1938) 391.
28. J. Tafel, *Z. Phischem.* **50** (1904) 641.
29. V.C. Levich, 'Physicochemical Hydrodynamics', (Prentice Hall, Englewood Cliffs, NJ, 1962).